The role of positron emission tomography-computed tomography/magnetic resonance imaging in the management of sarcoidosis patients

Chetsadaporn Promteangtrong[1, 2] MD, Ali Salavati[1] MD MPH, Gang Cheng[1] MD PhD, Drew A. Torigian[1] MD MA, Abass Alavi[1] MD, MD (Hon), PhD (Hon), DSc(Hon)

1. Department of Radiology, University of Pennsylvania, and Hospital of the University of Pennsylvania, Philadelphia, USA.
2. National Cyclotron and PET Center, Chulabhorn Hospital, Bangkok, Thailand

Keywords: Lymphoma
Sarcoidosis - PET/MRI
- Occult sarcoidosis
- Management

Correspondence address:
Abass Alavi, MD, PhD (Hon.), DSc (Hon.), MD (Hon.)
Department of Radiology, Hospital of the University of Pennsylvania 3400 Spruce Street, Philadelphia, PA 19104; USA
Phone: 215-662-3069
Fax: 215-573-4107
E-mail: abass.alavi@uphs.upenn.edu

Received:
21 July 2014
Accepted:
28 July 2014

Abstract
Sarcoidosis is a multisystem granulomatous disease of unknown etiology. The diagnosis is based on clinical and radiographic findings as well as by histopathological findings. Molecular imaging in recent years has made important progress regarding the study of various inflammatory diseases including sarcoidosis. Positron emission tomography (PET) provides an insight in metabolism of this disease. Positron emission tomography with fluorine-18-fluorodeoxyglucose (^{18}F-FDG) has shown effectiveness in detecting occult disease and assessing disease activity during treatment. This review article provides an overview of the applications of PET/computed tomography and PET/ magnetic resonance imaging for evaluation of patients with sarcoidosis.

Hell J Nucl Med 2014; 17(2): 123-135 *Published online: 7 August 2014*

Introduction

Sarcoidosis is a multisystemic disorder of unknown etiology with the pathological characteristic of non-caseating epithelioid cell granuloma formation. It was first described by Jonathan Hutchinson in 1877, but was termed "sarkoid" in 1899 by Caesar Boeck who described a patient with cutaneous lesions which he felt were similar to sarcoma, but were benign [1, 2]. The epithelioid cell granulomas is composed of highly differentiated mononuclear lymphocytes and phagocytes, with fibrotic change beginning from the periphery and progressively extending to the central part [1].

Sarcoidosis occurs worldwide affecting both men and women of all ages and races with variable incidence, manifestations, and prognosis. The highest annual incidence is observed in northern European countries [3] and in African Americans [4]. The disease tends to affect adults less than 40 years old, peaking in the second decade of life. In Japan and Scandinavian countries, a second peak incidence is found in females greater than 50 years of age [1].

The diagnosis is based on clinical and imaging features, histological confirmation, and exclusion of other diseases that can create similar histopathological and clinical findings. The clinical presentation can vary from incidental detection in asymptomatic patients to slowly progressive disease that involves any organ. The thorax is involved in up to 90% of patients with sarcoidosis [5], typically with bilateral hilar lymphadenopathy seen on chest radiographic examination. The most common clinical presentations are cough and dyspnea due to pulmonary involvement. Skin involvement can present in various form such as erythema nodosum, maculopapular lesions, subcutaneous nodules, and lupus pernio [6]. Patients may present with hepatomegaly, cholestasis, portal hypertension, lymphopenia, anemia, hypercalcemia, or diabetes insipidus. The majority of patients with sarcoidosis have a favorable outcome as granulomas disappear overtime and respond to corticosteroid treatment. Remission occurs in more than 50% of patients within 3 years of diagnosis, and within a decade for two-thirds of patients with no or few clinical consequences. Up to 33% of patients have persistent disease, leading to significant organ impairment [5, 7]. Besides obtaining a full patient history and performing a physical examination, recommended investigations for initial evaluation of sarcoidosis include chest radiography, pulmonary function testing, peripheral blood counts, serum chemistries, urinalysis, electrocardiography, eye examination, tuberculin skin testing, and bronchoalveolar lavage. Endobronchial ultrasonography-guided transbronchial needle aspiration (EBUS-TBNA) has also been used as a minimally invasive diagnostic procedure [8, 9]. In recent years, positron emission tomography (PET) and cardiac magnetic resonance imaging (MRI) have been suggested as effective imaging

tools in the evaluation of patients with sarcoidosis [10-13]. In this review, we will discuss the utilities of PET or PET/computed tomography (CT) and PET/MRI in sarcoidosis.

The role of ^{18}F-FDG PET/CT and MRI in sarcoidosis

Immunopathology of sarcoidosis and glucose metabolism

T-helper 1 (Th1) cells play a major role in immune response of sarcoidosis. Antigen is presented by major histocompatibility complex class II leading to activation of Th1 cells and subsequent production of various types of cytokines and chemokines including interferon-γ, transforming growth factor β, tumor necrosis factor-α,interleukin (IL)-2, IL-12, and others [5, 14]. The immune response then leads to the granuloma formation, which consists of a central core of mononuclear cells surrounded by CD4 cells and a small number of CD8 and B cells [4]. There is evidence that cells have increased glucose metabolism during the inflammatory process. Metabolic changes of inflammatory cells, such as T-helper cells and activated macrophages, enhance the glucose uptake, glycolysis, and increased pentose phosphate pathway activity [15].

Tissues with high glucose metabolism such as brain tissue gray matter, cancer cells, and inflammatory changes show increased fluorine-18 fluorodeoxyglucose (^{18}F-FDG) accumulation on PET imaging. As a key component of the inflammatory process, inflammatory cells consume glucose at a much higher level than peripheral non-inflammatory cells, leading to higher glucose metabolism and increased uptake of ^{18}F-FDG within inflammatory foci. Studies have demonstrated that ^{18}F-FDG is accumulated by leukocytes and macrophages in vitro [16, 17], as well as in sites of inflammation [18, 19]. Recently, ^{18}F-FDG PET/CT has been used in to assess a wide variety of inflammatory diseases such as vasculitis [20], atherosclerosis [21, 22], arterial wall inflammation in HIV infection [23], cardiac valvular inflammation [24], arthritis [25], radiation pneumonitis [26], and febrile neutropenia [27].

Fluorine-18-FDG PET for detection and response assessment of sarcoidosis

Lung is the most common site of organ involvement by sarcoidosis, and is present in 90% of patients [5, 28]. Extrathoracic manifestations are present in 25%-50% of the patients, typically in combination with thoracic disease [28]. Chest radiography is the most common imaging technique used in sarcoidosis and is abnormal in 80%-90% of cases. The sarcoidosis Scadding staging system (Table 1) depends on presence of hilar lymph node enlargement and pulmonary opacities on chest radiography [29]. Classic stage I disease consisting of bilateral hilar lymphadenopathy without parenchymal disease is the most common initial presentation. Stage II consists of hilar or mediastinal lymphadenopathy with parenchymal opacity. Stage III entails parenchymal involvement without lymphadenopathy. Stage IV shows evidence of pulmonary fibrosis. Normal chest radiography is considered to be stage 0. The high-resolution CT (HRCT) is able to demonstrate abnormal lung parenchyma [30]. Findings of HRCT sarcoidosis may include hilar and/or mediastinal lymph node enlargement (sometimes with calcification), pulmonary interstitial nodules in a perilymphatic distribution, thickening of the peribron chovascularinterstitium, pulmonary ground glass opacity, consolidation, or large nodular opacities, and coarse linear opacities, interlobular septal thickening, honeycombing, cysts, architectural distortion, superior hilar retraction, or traction bronchiectasis related to fibrosis. Pleural disease is rare and may be observed when disease is extensive.

Table 1. *Scadding staging system on chest radiograph*

Scadding stage	Radiographic finding
0	Normal
I	Bilateral hilar lymphadenopathy without parenchymal disease
II	Bilateral hilar lymphadenopathy with parenchymal disease
III	Parenchymal disease without hilar lymphadenopathy
IV	Pulmonary fibrosis

Gallium-67 citrate (^{67}GaC) scintigraphy has historically been widely used in sarcoidosis, which provides advantages of functional assessment and whole body evaluation [28, 31]. There is a typical pattern of ^{67}GaC uptake in sarcoidosis, called the "lambda" sign, which is due to radiotracer uptake in bilateral hilar and right paratracheal lymph nodes. There is also a "panda" sign due to radiotracer uptake in the lacrimal glands, parotid glands, and nasal mucosa, which is nonspecific since it is also found in other conditions such as acquired immunodeficiency syndrome (AIDS), Sjögren's syndrome, following irradiation of the head or neck, particularly for lymphoma treatment [31-33]. The "lambda" sign with an associated "panda" sign is highly specific for sarcoidosis, even in patients with normal chest radiography and CT or in pa-

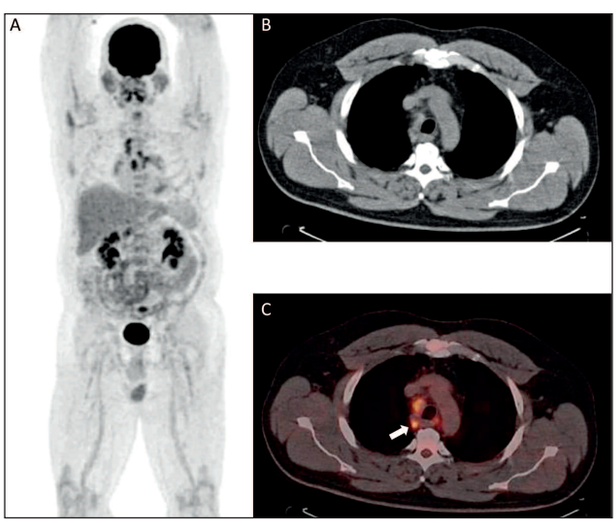

Figure 1. A 49 years old man with sarcoidosis. (A) Whole-body ^{18}F-FDG PET image shows cardiac, mediastinal, and hilar lymph node involvement of sarcoidosis. (B) Axial fusion PET/CT show increase ^{18}F-FDG uptake at mediastinal lymph nodes (arrow).

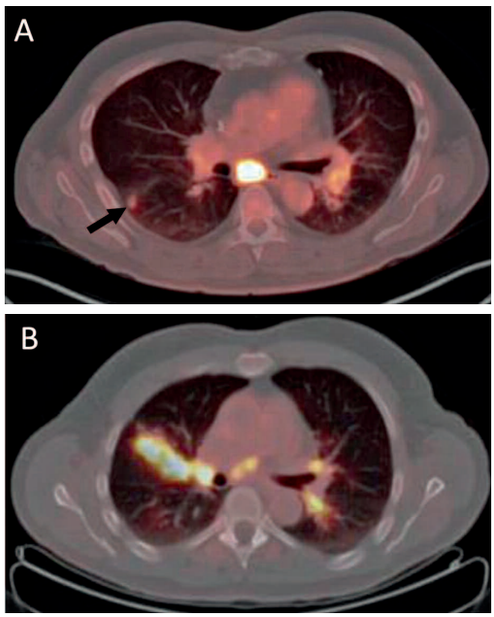

Figure 2. A) A 51 years old man with sarcoidosis. Increased uptake at subcarina and left hilar lymphadenopathy. A hypermetabolic right lung nodule was also noted (black arrow). B) A 65 years old man with sarcoidosis. Increased uptake at right upper lobe associated with interstitial nodules with perilymphatic/peribronchovascular distribution. Increased uptake at mediastinal and bilateral hilar lymphadenopathy was noted.

tients with non-diagnostic hilar lymphadenopathy [34]. However, the use of ^{67}GaC scintigraphy has decreased due to its limitations. The overall sensitivity and specificity vary with significant inter observer variability. The radiotracer distribution time requires at least 48-72h prior to image acquisition [28, 35, 36].

Functional imaging of sarcoidosis has more recently been performed with ^{18}F-FDG PET/CT due to its improved image resolution, the relatively short delay time between radiotracer injection and image acquisition, and improved anatomical localization of sites of abnormality. The sensitivity of ^{18}F-FDG PET/CT in detecting active sarcoidosis is 80%-100% [34]. The findings of sarcoidosis on ^{18}F-FDG PET/CT are similar to those seen on ^{67}GaC imaging. Figure 1 shows ^{18}F-FDG PET images of a sarcoidosis patient with cardiac, mediastinal lymph node, and hilar lymph node involvement. Figure 2 shows PET, CT and fusion PET/CT images of patients with pulmonary involvement. Lewis et al. presented in 1994 the initial study that described ^{18}F-FDG uptake within intra- and extra-thoracic sarcoidosis [37]. The investigators reported two cases of sarcoidosis in which ^{18}F-FDG PET can identify sarcoidosis lesions. The first patient underwent whole-body ^{18}F-FDG PET scan due to suspected lymphoma, which revealed multiple areas of intense ^{18}F-FDG uptake in sites including bilateral hilar and paratracheal regions, paraaortic region, bilateral cervical regions, bilateral inguinal regions, left axilla, right hepatic lobe, and spleen, while histopathology findings from mediastinal lymph node biopsy revealed granulomas without malignant cells, caseation, or acid fast bacilli. The other patient described in this report had erythema nodosum and bilateral hilar lymphadenopathy on chest radiography. The ^{18}F-FDG PET scan of the second patient demonstrated markedly increased ^{18}F-FDG uptake in the hilar and paratracheal regions with patchy superficial radiotracer uptake seen in both lower limbs, which subsequently resolved at follow-up ^{18}F-FDG PET imaging obtained 3 months after oral corticosteroid therapy.

Nishiyama et al (2006) [36] compared ^{18}F-FDG PET to ^{67}GaC scintigraphy and single photon emission tomography (SPET) of the thorax in 18 patients with sarcoidosis. Pulmonary and extrapulmonary lesions were evaluated and confirmed by histopathology or radiological findings scintigraphy with ^{18}F-FDG PET and ^{67}GaC single photon emission tomography (SPET) of thorax detected 100% and 81%, respectively of intrapulmonary sites. For extrapulmonary sites, ^{18}F-FDG PET and ^{67}GaC scintigraphy detected 90% and 48%, respectively.

Braun et al (2008) [38] retrospectively studied ^{18}F-FDG PET/CT in 20 patients with histological confirmation of intra- and extra-thoracic sarcoidosis. Twelve patients underwent both ^{18}F-FDG PET/CT and ^{67}GaC scintigraphy including whole body planar and thoracic and abdominopelvic SPET. The investigators showed good ^{18}F-FDG PET/CT sensitivity, greater than ^{67}GaC scan sensitivity, for detection of active foci of thoracic (100% vs. 71%), pharyngolaryngeal (80% vs. 67%), and sinonasal (100% vs. 75%) disease. They suggested that small cutaneous or subcutaneous sites of disease, including lupus pernio, were very difficult to appreciate on scintigraphic images, especially when anatomical structures with physiologic or pathological radiotracer accumulation were superimposed. Considering all extra-cutaneous biopsy-proven sites of sarcoidosis localization, the overall sensitivity of ^{18}F-FDG PET/CT and ^{67}GaC scan was 87% and 67%, respectively.

Positron emission tomography can be used as a useful tool for the diagnosis of sarcoidosis by identifying potential biopsy sites in organs that might be accessible. Figure 3 (A-B) shows ^{18}F-FDG PET images of a patient with bone marrow involvement. Figure 3 (C-D) shows ^{18}F-FDG PET images of a patient with splenic involvement. Figure 4 shows PET, CT and fusion ^{18}F-FDG PET/CT of sarcoidosis lesions at bilateral iliac and right sacro-iliac joint. A study by Teirstein et al (2007) [39] reviewed the use of ^{18}F-FDG PET in 137 patients diagnosed with sarcoidosis to evaluate its role in the identification of occult biopsy sites and reversible granulomatous disease. One hundred thirty-nine of 188 scans showed positive findings, where the most common sites were the mediastinal lymph nodes (54 scans), extra-thoracic lymph nodes (30 scans), and lung parenchyma (24 scans). In 20 patients, ^{18}F-FDG PET indicated the presence of active extracardiac disease that was not detected by physical examination, chest radiography, or CT, leading to a diagnostic biopsy in five patients. Eleven follow-up ^{18}F-FDG PET scans after corticosteroid therapy showed a decreased standardized uptake value (SUV) of lymph nodes, lungs, spleen, lacrimal glands, skin, and bones. In most cases, symptoms, conventional imaging, and physiological data paralleled the improvement seen on PET scans. Positron emission tomography also showed positive pulmonary finding in two thirds of patients, which was common in patients with stage II and III disease. Patients with stage 0, I, and IV disease commonly do not have significant pulmonary PET findings. However, there was no correlation between positive PET scan findings and lung diffusing capacity

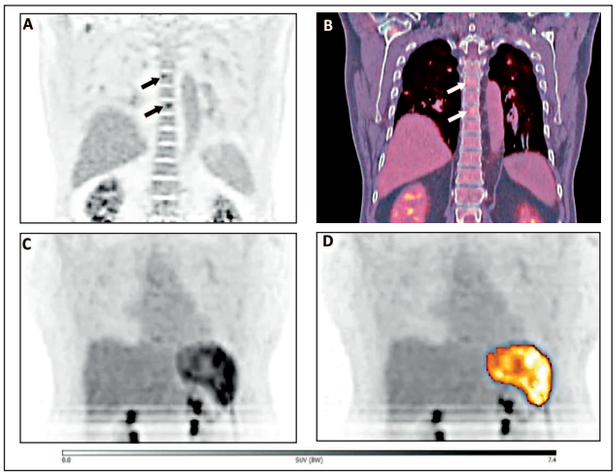

Figure 3. A) ^{18}F-FDG PET showed two foci of bone marrow involvement by sarcoidosis at vertebral bodies (arrows), B) Coronal fusion PET/CT. C) Maximum intensity projection of ^{18}F-FDG PET showed sarcoidosis involvement at spleen, D) PET after segmentation of splenic lesion.

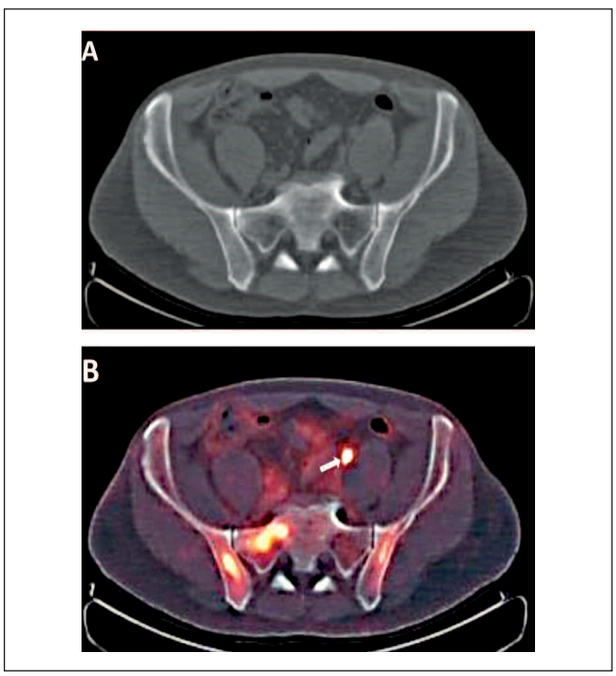

Figure 4. A 65 years old man with sarcoidosis. A) Axial CT image B) Axial fusion ^{18}F-FDG PET/CT showed increased uptake at bilateral iliac and right sacro-iliac joint. Focal activity in left ureter was noted (white arrow).

for carbon monoxide (DLCO) or serum angiotensin-converting enzyme (ACE) levels.

Mostard et al (2011) [40] retrospectively studied ^{18}F-FDG PET/CT findings compared to levels of ACE, soluble IL-2 receptor (sIL-2R) and neopterin (a marker for immune system activation) in 89 patients with disabling symptoms related to sarcoidosis. Sixty-five (73%) patients had a positive PET/CT scan, 52 with serological signs of inflammatory activity. PET/CT was positive in 14/15 patients with stage IV sarcoidosis. In 80% of PET/CT positive patients, extrathoracic inflammatory activity was found. The sensitivity of combined serological markers for the presence of disease activity was 80% with a specificity, positive predictive value, and negative predictive value of 100%, 100% and 65%, respectively. These findings suggest that PET/CT appears to be of additional value in depicting disease in patients with persistent symptoms in the absence of increased serum markers as well as in detecting extra thoracic lesions.

For restaging and follow-up, recent study by Rubini et al (2014) [41] found sensitivity, specificity and accuracy of PET/CT of 100%, 50% and 87.5%, respectively while MDCT provided sensitivity, specificity and accuracy of PET/CT of 91.67%, 81.25% and 50%, respectively. The responsiveness of PET/CT after treatment were in agreement with the change of clinical status as perceived by the patients [42].

Disease activity assessment by ^{18}F-FDG PET

Fluorine-18-FDG PET has been studied for the purpose of evaluating disease activity. Patients' symptoms and objective parameters may differ in reflecting the level of disease activity of sarcoidosis, and there is no reference standard to define disease activity in patients with this disease. Follow-up for sarcoidosis includes history, chest radiography, pulmonary function testing, and serum biomarkers. Symptoms may be difficult to interpret. Chest radiography and HRCT are suboptimal for revealing active inflammation [43]. Although HRCT is useful to provide information regarding the presence and distribution of pulmonary abnormalities, the findings do not correlate better than radiography findings with measures of clinical and functional impairment [44]. An improvement of pulmonary functional test results reflects a positive treatment response, although persistent abnormal results might be found in both ineffective treatment and irreversible fibrotic change. Angiotensin- converting enzyme (ACE) produced within granulomas by epithelioid cells and alveolar macrophages through the release of an ACE-inducing factor may be used to monitor disease activity. However, the ACE level is above normal limits in only 60% of patients with chronic sarcoidosis and is unrelated to disease severity, progression, clinical course, and response to therapy [43], and is also present in other granulomatous conditions. Another marker is sIL-2R, which is released by T cells. It is an accurate biomarker for the assessment of pulmonary sarcoidosis and correlates with presence of active disease, although it is still not recommended for use as an activity biomarker [45]. Both ACE and sIL-2R may not be sensitive enough and may not correlate with patients' symptoms and levels of functional impairment.

Keijsers et al (2009) [46] retrospectively reviewed ^{18}F-FDG PET and levels of ACE and sIL-2R in 36 newly diagnosed sarcoidosis patients. The serum markers were obtained within 4 weeks of ^{18}F-FDG PET. The authors determined the sensitivity of ^{18}F-FDG PET in active sarcoidosis and its correlation with other markers. Positron emission tomography was found to be positive in 94% of patients. Thirteen patients (36%) showed an increased ACE level and seventeen patients (47%) showed an increased sIL-2R level. Increased ACE and sIL-2R levels correlated with positive ^{18}F-FDG PET findings in 12 patients (92%) and 16 patients (94%), respectively. However, there was no correlation between SUV measurements and ACE or sIL-2R levels. SIL-2R and ACE levels had a low diagnostic performance for the detection of active sarcoidosis, although sIL-2R and

positive ACE levels correlated well with ^{18}F-FDG PET. Therefore, ^{18}F-FDG PET could be excluded when these serum markers are increased. The authors also suggested a potential future role for ^{18}F-FDG PET in sarcoidosis assessment.

The same group (2010) [47] compared bronchoalveolar lavage (BAL) cell profile and ^{18}F-FDG PET in 77 newly diagnosed pulmonary sarcoidosis to evaluate whether metabolic activity on PET represented disease activity as assessed by BAL. They categorized patients based on ^{18}F-FDG PET as exclusively mediastinum/hilar activity (Group A) and activity in lung parenchyma (Group B). Bronchoalveolar lavage lymphocyte (%), CD103+CD4+/CD4+ ratio, CD4/CD8 ratio and neutrophils percentage were compared with measurements of metabolic activity calculated by SUVmax. Overall SUVmax in the lung parenchyma showed significant correlation with the percentage of neutrophils. CD4/CD8 ratio significantly correlated with the SUVmax of the mediastinum. They also found a positive correlation between SUVmax of the lung parenchyma and radiographic stage, and a negative correlation between SUVmax of mediastinum and radiographic stage. In radiographic stages 0 and IV, ^{18}F-FDG PET showed active lesions in the mediastinum/hila of all patients and parenchymal activity in 57%. Even in stage I disease, increased metabolic activity in the lung parenchyma was seen in 52% of patients. They proposed that conventional chest radiography staging does not appear to be as reliable as currently thought for determining disease activity.

Another study by Keijsers et al (2008) [48] compared ^{18}F-FDG-PET results with sarcoidosis parameters following treatment with infliximab, an anti-TNF-α therapy. Twelve patients with refractory sarcoidosis were treated with 6 cycles of infliximab and underwent pre- and post- treatment ^{18}F-FDG PET. Effect of treatment was also evaluated by change in symptoms, ACE levels, sIL-2R levels, vital capacity (VC), DLCO levels, and chest radiographic findings. Eleven patients noticed an improvement of symptoms with no improvement on chest radiography. One patient, who did not observe an improvement, had pulmonary function test results that remained at the same level and serum markers that showed a dramatic decrease. The decrease in ACE and sIL-2R levels was 39% and 47%, respectively. Improvements of VC and DLCO were by 5.4% and 3.3%, respectively. ^{18}F-FDG PET showed either improvement or normalization of metabolic abnormalities in 11/12 (92%) of clinically responding patients. The overall decrease in SUVmax was 55%. However, they did not find a significant correlation between SUVmax and other parameters except VC. These findings support the hypothesis that ^{18}F-FDG uptake represented disease activity with a higher sensitivity than other parameters.

Sobic-Saranovic et al (2012) [43] studied 90 sarcoidosis patients who had persistent symptoms. Patients underwent ^{18}F-FDG PET/CT and CT together with measurement of ACE levels. During follow-up assessment (12±5 months after ^{18}F-FDG PET/CT), clinical status and changes in therapy were analyzed. ^{18}F-FDG PET/CT detected inflammation in 82% of patients while CT was positive in 6 additional patients (89%). However, the difference between two methods was not significant (P=0.238) and their agreement was fair (k=0.198). Isolated extrathoracic sarcoidosis was found in 5 patients only on ^{18}F-FDG PET/CT. Retroperitoneal and cervical lymph nodes were the most frequent extrathoracic sites found on PET/CT, followed by skin, parotid glands, and adrenal glands. Angiotensin-converting enzyme levels were significantly higher in patients with positive than negative ^{18}F-FDG PET scan findings, but 51% of patients with positive PET results had normal ACE levels. In both univariate and multivariate logistic regression analyses the positive ^{18}F-FDG PET/CT studies were significantly associated with changes in therapy, with no impact from age, sex, CT, ACE levels, or previous treatments. They concluded that ^{18}F-FDG PET/CT is a useful adjunct to other diagnostic methods for detecting active inflammatory sites in patients with chronic sarcoidosis with persistent symptoms, especially in those with normal ACE levels. ^{18}F-FDG PET/CT also proved advantageous for determining the spread of active disease throughout the body and influenced patient management.

Other study of Mostard et al (2013) [49] found the relationship between the severity of pulmonary sarcoidosis and increased PET activity in patients with persistent symptoms. The severity of pulmonary involvement was assessed by HRCT and pulmonary function tests. All patients with FVC <50% or DLCO <45% showed PET-positive findings. Interestingly, 85% of patients with signs of fibrosis on HRCT had PET positivity and of whom 82% showed extrathoracic PET activity and 73% had increased serological inflammatory markers.

Ambrosini et al (2013) [50] assessed sarcoidosis activity and extension in comparison with thoracic HRCT in 28 patients and 35 PET/CT scans. On a scan basis, PET/CT was concordant with HRCT in 16 scans (45.7%), detecting active disease in 10 scans and no activity in 6 scans. In 19 (54.3%) discordant scans, PET/CT was positive in 14 scans, active lung disease with nodal involvement in 1 scan, indicating active nodal disease in 3 scans, active lung and/or nodal disease with extrapulmonary disease in 9 scans, and disease relapse at extrapulmonary level without lung involvement in 1 scan. PET/CT information influenced the clinical management in 22 (63%) of 35 scans. This study supported the use of ^{18}F-FDG PET/CT to assess sarcoidosis activity and spatial extent to obtain valuable information for the clinical management. PET/CT detection of unsuspected activity in the lungs of patients with nodal sarcoidosis or the identification of extrapulmonary activity may help in clinical decision making, especially with regards to whether treatment should be initiated.

Fluorine-18-FDG PET in cardiac sarcoidosis

Cardiac involvement is clinically detected in 5% of sarcoidosis patients and in 40% of patients at autopsy [4]. Complications of cardiac sarcoidosis include conductional abnormalities, ventricular tachycardia, congestive heart failure, and sudden cardiac death. Therefore, cardiac involvement is an important prognostic factor in patients with sarcoidosis [45]. Besides a history and physical examination, electrocardiography (ECG) and transthoracic echocardiography are useful for cardiac evaluation. Cardiac MRI and cardiac ^{18}F-FDG PET have emerged as well for this purpose in recent clinical practice. Management of cardiac sarcoidosis includes immunosuppressive therapy, dysrhythmia management, and management of underlying left ventricular dysfunction. Some patients may also require pacemaker and defibrillator placement.

Histological biopsy of the myocardium is the reference standard for diagnosis of cardiac sarcoidosis, however its sensitivity is only 20%-30% [51]. Cardiac MRI is a sensitive technique to assess the locations and extent of disease. Myocardial sarcoidosis may present on cardiac MRI as segmental wall motion abnormality, focal wall thickening or thinning, or nodules with a patchy distribution. Delayed phase contrast enhancement may also be seen, related to the presence of fibro granulomatous tissue [34]. However, it is not easy to differentiate between active and inactive sarcoidosis lesions, which is important for patient management. In addition, cardiac MRI is generally contraindicated in patients with pacemakers or defibrillators. Recent clinical diagnostic criteria for cardiac sarcoidosis have been established by the Japanese Ministry of Health and Welfare in 2006 [52], which include ^{67}GaC scintigraphic findings under the major criteria and thallium-201 (^{201}Tl) or technetium-99m (^{99m}Tc) SPET under the minor criteria without mention of ^{18}F-FDG PET imaging.

A number of studies have evaluated the utility of ^{18}F-FDG PET in diagnosing cardiac sarcoidosis [36, 53-57]. A summary of these studies is shown in Table 2. A recent systematic review by Youssef et al (2012) [12] found that ^{18}F-FDG PET has pooled sensitivity of 89% and specificity of 78%. However, the specificities had significant heterogeneity, as was apparent from a high inconsistency index (71.7%) and a wide range (38%-100%). Irrespective to the causes of the heterogeneity, the overall consistency of high sensitivity did suggest that a negative result can exclude cardiac involvement with high confidence. Figure 5(A-D) shows PET and PET/CT images of patients with cardiac sarcoidosis. Figure 5(E-H) shows PET and PET/CT images of cardiac sarcoidosis patient who also has mediastinal and hilar lesions.

Ohira et al (2008) [53] compared ^{18}F-FDG PET and cardiac MRI for detection of cardiac sarcoidosis in 21 patients with suspected cardiac sarcoidosis. The sensitivity and specificity of ^{18}F-FDG PET were 87.5% and 38.5%, respectively, whereas those of cardiac MRI were 75% and 76.9%, respectively. One explanation for the low specificity of PET was that the study only enrolled patients with suspected cardiac sarcoidosis. Another explanation was that nonspecific ^{18}F-FDG uptake in myocardium was observed in this study, although this was felt to be unlikely given the lack of nonspecific uptake in control subjects from a previous study [56] which used the same imaging protocol. The authors hypothesized that ^{18}F-FDG PET detected early-stage sarcoidosis lesions in the heart even in patients who did not meet the diagnostic criteria. The presence of positive findings on ^{18}F-FDG PET was associated with elevated serum ACE levels; this association was not demonstrated on MRI. With cardiac sarcoidosis, focal ^{18}F-FDG uptake in heart is thought to reflect the presence of accumulated inflammatory cells, whereas high signal intensity on T2 weighted image of cardiac MRI represents edema and/or increased extracellular space.

Some studies have addressed the value of ^{18}F-FDG PET or PET/CT for assessment of myocardial sarcoidosis activity after treatment [58-60]. Fluorine-18-FDG PET is useful to determine whether continued antiarrhythmic drug therapy or corticosteroid treatment is necessary. Fluorine-18-FDG PET/CT

***Table 2**. Sensitivity and specificity of ^{18}F-FDG PET for diagnosis of cardiac sarcoidosis*

Study/ Year	No. of patients	Sensitivity (95% CI)	Specificity (95%CI)
Langah et al. 2009 [49]	30	0.85 (0.62-0.97)	0.90 (0.55-1.00)
Ohira et al 2008 [48]	21	0.88 (0.47-1.00)	0.38 (0.14-0.68)
Nishiyama et al. 2006 [35]	18	1.00 (0.59-1.00)	1.00 (0.72-1.00)
Ishimaru et al.2005 [51]	32	1.00 (0.48-1.00)	0.81 (0.62-0.94)
Okumura et al. 2004 [50]	22	1.00 (0.72-1.00)	0.91 (0.59-1.00)
Yamagishi et al. 2003 [52]	17	0.82 (0.57-0.96)	Could not determine

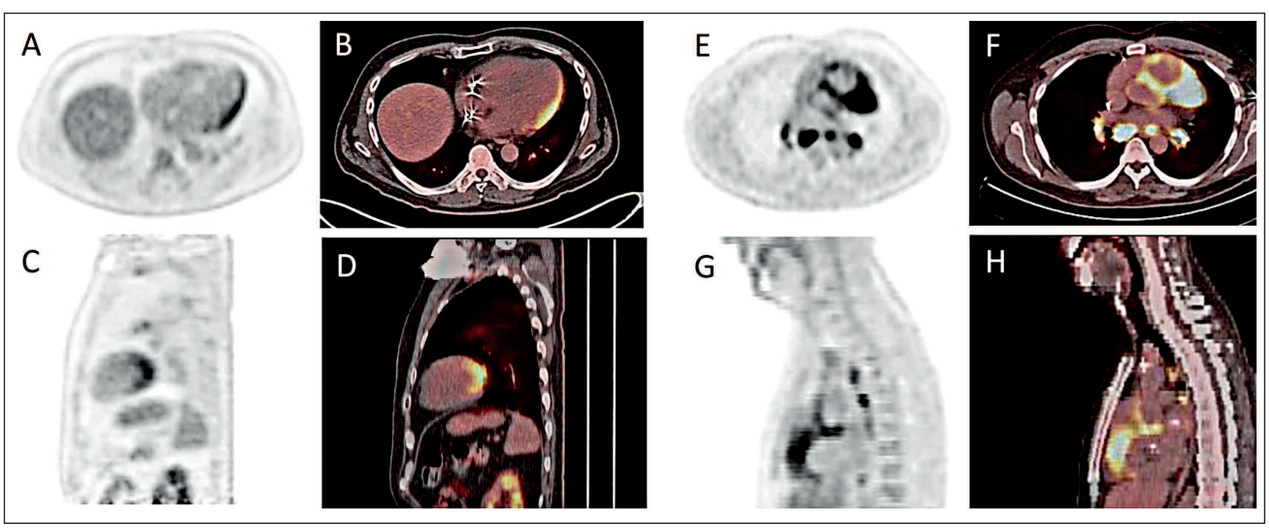

Figure 5. (A-D) A 50 years old man with cardiac sarcoidosis. Axial and sagittal fusion ^{18}F-FDG PET/CT showed increased uptake at lateral wall of left ventricle. (E-H) A 47 years old man with sarcoidosis. Axial and sagittal fusion ^{18}F-FDG PET/CT showed increased uptake at myocardium, mediastinal and hilar lymphadenopathy.

showed more predictable information about disease reversibility compared to cardiac MRI [59]. Takeda et al (2002) [61] reported resolution of ^{18}F-FDG uptake on follow-up PET imaging after corticosteroid therapy in patients with cardiac sarcoidosis. Figure 6 shows baseline and follow-up ^{18}F-FDG PET images from patients with cardiac, pulmonary and mediastinal lymph node involvement by sarcoidosis. Figure 7 shows baseline and follow-up ^{18}F-FDG PET images from a patient with splenic involvement bysarcoidosis.

Fluorine-18-FDG PET is a valuable tool for the diagnosis of cardiac sarcoidosis. Focal hypermetabolic activity or a focal increase of activity with a diffusely increased background on ^{18}F-FDG PET is characteristic for cardiac sarcoidosis. However, this technique has some limitations. Normal myocardial cells use glucose as one of main energy substrates, and so physiologic ^{18}F-FDG uptake in the myocardium may variably be found in healthy subjects. Papillary muscles and the lateral wall of the left ventricle may also show normal focal uptake of ^{18}F-FDG. For optimal ^{18}F-FDG PET imaging in cardiac sarcoidosis, minimization of glucose uptake by normal myocardium is necessary to ensure high contrast between lesions and the normal background. Special patient preparation is therefore needed prior to ^{18}F-FDG PET imaging to evaluate cardiac sarcoidosis. There are three approaches available for this purpose: prolonged fasting, dietary modification with a low-carbohydrate and high-fat diet, and intravenous administration of unfractionated heparin. These approaches are used to promote free fatty acid metabolism and to suppress ^{18}F-FDG uptake [62]. It is possible that a combination of all of these techniques may be superior to any one alone [63]. Morooka et al (2014) [64] found higher effect in inhibiting myocardial uptake of an 18h fast than heparin loading plus a 12h fast before scan. They also found the association between high level of free fatty acid and reduction of physiologic myocardial uptake. The investigators suggested the monitoring free fatty acid levels may improve PET interpretation of active cardiac sarcoidosis.

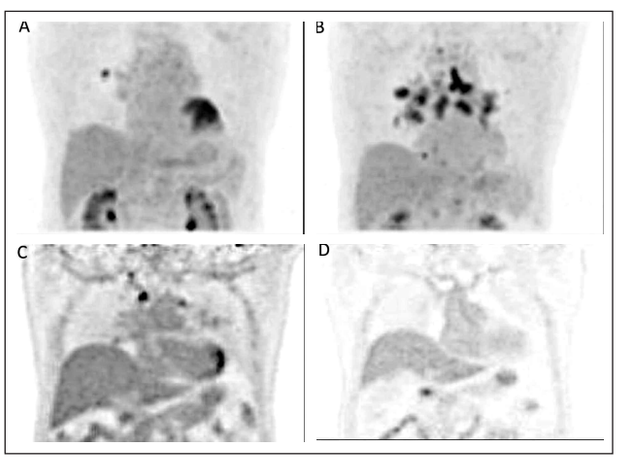

Figure 6. A) Maximum intensity projection ^{18}F-FDG PET with segmentation of a 75 years old man diagnosed cardiac sarcoidosis. Baseline scan showed extensive ^{18}F-FDG uptake at left ventricle and pulmonary nodule at right upper lung. B) Seven months after prednisolone treatment, there was no active cardiac inflammation. However, there was progression of pulmonary and lymph node involvement. C) Baseline ^{18}F-FDG PET scan showed ^{18}F-FDG uptake at left ventricle and lymph nodes. D) Seventeen months after prednisolone and TNF inhibitor treatment, follow-up scan showed no active sarcoidosis lesion.

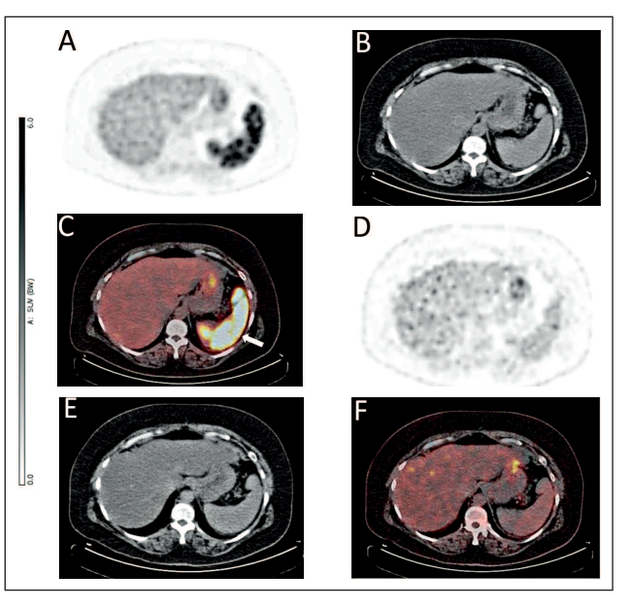

Figure 7. A 49 years old woman with sarcoidosis. A-C) Baseline PET/CT images showed increase ^{18}F-FDG uptake at spleen. D-F). Nine months after prednisolone and methotrexate treatment, follow-up axial PET/CT images showed resolution of splenic lesion.

Fluorine-18-FDG PET in neurosarcoidosis

Neurosarcoidosis affects 5%-15% of patients with sarcoidosis. The cranial nerves are the most commonly affected site, although any part of nervous system can be involved. The most common cranial nerve involved is the facial nerve presenting as facial palsy, followed by the optic nerve presenting as diplopia or impaired visual acuity. Symptoms and signs of neurosarcoidosis may include cranial neuropathy, meningeal irritation, increased intracranial pressure, peripheral neuropathy, pituitary and hypothalamic dysfunction, cognitive dysfunction, and personality change. Neurosarcoidosis can occasionally be life-threatening as well [4].

Contrast-enhanced MRI for detection of intracranial and spinal cord lesions is the imaging modality of choice for evaluating neurosarcoidosis. However, the findings on MRI are often nonspecific. Electromyography (EMG) can be useful for peripheral neuropathy evaluation, although the findings are also nonspecific. Interpretation of ^{18}F-FDG PET in neurosarcoidosis may be difficult because of physiologic uptake of ^{18}F-FDG activity in normal gray matter. Moreover, granulomatous inflammation shows hypermetabolism whereas neuronal damage presents as hypometabolism. ^{18}F-FDG PET may reveal additional occult lesions amenable to biopsy in some patients with inaccessible intracranial lesions. However, the literature on ^{18}F-FDG PET and neurosarcoidosis is extremely limited (Fig. 8). A few case reports relevant to the application of ^{18}F-FDG PET or PET/CT in patients with neurosarcoidosis have been reported in the literature [65-72]. For example, Huang et al [71] demonstrated abnormal ^{18}F-FDG uptake at spinal level T9-T12 but a normal MRI of thoracolumbar region in a patient with sarcoidosis who had symptoms of band like abdominal pressure and urinary frequency.

Sakushima et al (2011) [73] compared the SUVs measured on ^{18}F-FDG PET of spinal cord sarcoidosis lesions and non-inflammatory spinal cord lesions in 3 patients with spinal

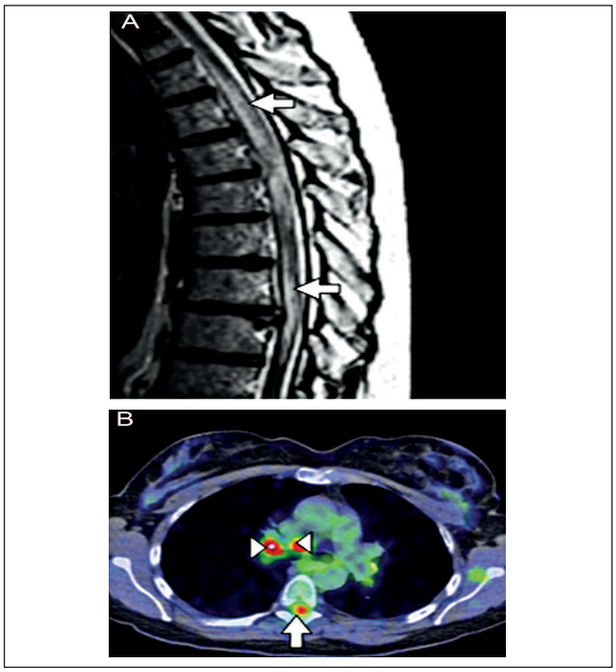

Figure 8. A patient with neurosarcoidosis. A) MRI of thoracic cord shows longitudinally extensive T2 signal hyperintensity (arrows). B) Increased ^{18}F-FDG uptake in corresponding location (red color) (arrow; SUVmax, 6.3g/mL) and additional ^{18}F-FDG PET hypermetabolism of perihilar lymph nodes (arrowheads). (Reprinted and modified, with permission, from reference 72).

cord sarcoidosis, five patients with myelomalacia caused by cervical spondylosis or ossification of the posterior longitudinal ligament, one patient with spinal cord edema from cervical degenerative disease, and one patient with spinal cord edema due to a dural arteriovenous fistula. Significantly higher SUVs were found in spinal cord sarcoidosis lesions (mean 4.38, range 3.30-4.93) compared to those of the other spinal cord lesions (mean 1.87, range 1.42-2.74). The authors concluded that ^{18}F-FDG PET is informative and may be enable clinicians to start treatment at an earlier stage, as ^{18}F-FDG PET can detect early spinal cord involvement compared to MRI. Yet, more studies are needed to define the role of ^{18}F-FDG PET in patients with neurosarcoidosis.

Fluorine-18-FDG PET for prognostication of patient outcome in sarcoidosis

As the lung is the most commonly affected organ in sarcoidosis, pulmonary function test results, and in particular DLCO, may be abnormal. Keijser et al (2011) [74] used ^{18}F-FDG PET to study whether diffuse metabolic lung parenchymal activity could serve as a predictor of future pulmonary deterioration. They retrospectively studied 43 newly diagnosed sarcoidosis patients who underwent baseline and 1-year follow-up PET scans. They found a significant decrease in DLCO in untreated patients with diffuse parenchymal disease without change in vital capacity (VC) or forced expiratory volume in 1 second (FEV1). For the treated group with lung parenchymal activity, there was a significant increase in VC, FEV1, and DLCO whereas patients without parenchymal activity did not show any change in pulmonary function test results. The authors concluded that diffuse parenchymal disease in the ^{18}F-FDG PET scans predicts a future decline of DLCO when medical treatment is withheld.

Umeda et al (2011) [75] used dual-time-point ^{18}F-FDG PET to assess the prognosis, in terms of changes over time on serial CT scans, of patients with pulmonary sarcoidosis compared with ^{67}GaC scintigraphy and serum biomarkers. The retention index (RI), defined as (delayed SUV-early SUV)x100/ early SUV, was significantly greater in patients with increased or unchanged lung lesions at 1-year follow-up CT (persistent group; 21.3±9.6%) compared to patients with improved lung lesions (improved group; -9.2±28.6%, P=0.0075). The RI showed greater diagnostic accuracy in the persistent group than that of SUV based on early time point PET images (85.7% vs. 61.9%, P=0.034, McNemar test) or level of ^{67}GaC uptake (85.7% vs. 52.4%, P=0.0047). Serum sIL-2R levels showed a significant correlation with RI (r=0.698, P=0.0048) while serum ACE levels were not correlated with early time point SUV, delayed time point SUV, RI, or ^{67}GaC uptake. The authors suggested that ^{18}F-FDG PET may be a valuable biomarker of persistent inflammation in patients with pulmonary sarcoidosis.

Vorselaars et al (2014) [76] found that a mediastinal SUVmax ≥6.0 on ^{18}F-FDG PET at start of infliximab therapy was a significant predictor of relapse after discontinue treatment with hazard ratio of 4.33.

For cardiac sarcoidosis, abnormal myocardial uptake on ^{18}F-FDG PET can identify patients at higher risk of adverse events; death or sustained ventricular tachycardia [77]. Osborne et al (2014) [78] studied the association of serial PET imaging of cardiac sarcoidosis patients who had immunosuppressive treatments and their left ventricular ejection fraction (LVEF). There was an inverse linear relationship between SUVmax and LVEF with 7.9% increased LVEF per 10g.m/L SUV reduction (P=0.008). A mean increased in LVEF was 8.6%±5.2% in patients who responded to treatment while patients who did not respond to treatment had a mean decrease in LVEF of 5.5%±3.4%.

Other PET radiotracers for detection of sarcoidosis

Although ^{18}F-FDG PET is sensitive for detection of sarcoidosis, this method is not specific for this disease condition, as ^{18}F-FDG can be taken up by malignant cells and by inflammatory cells in other inflammatory disease conditions that may affect the lungs. Concomitant malignancy is found in 1.2 to 2.5% of patients with sarcoidosis [79, 80]. The main types of concomitant malignancy include lung cancer, lymphoma, testicular cancer, and uterine cancer [81]. Therefore, it may be difficult to use ^{18}F-FDG PET to evaluate sarcoidosis patients who have suspected malignancy or in cancer patients who have persistent bilateral hilar lymphadenopathy with lesions elsewhere in the body in remission. Thus, some studies have used non-^{18}F-FDG radiotracers with PET imaging to evaluate patients with sarcoidosis. Yamada et al (1998) [82] studied the role of ^{18}F-FDG and [^{11}C]-methionine (Met) as PET radiotracers for assessment of patients with pulmonary sarcoidosis. The accumulation of Met in tissues reflects increased amino acid transport and metabolism. In 31 patients, Yamada et al found overall sensitivities of both ^{18}F-FDG PET and Met-PET to detect thoracic lymphadenopathy of 97% (30/31 subjects). The mean level of ^{18}F-FDG uptake

was significantly higher than that of Met uptake. Patients were classified into an ^{18}F-FDG-dominant group (^{18}F-FDG/Met uptake ratio ≥2) and a Met-dominant group (^{18}F-FDG/Met <2). Without treatment after PET imaging, the ^{18}F-FDG-dominant group showed a significantly greater incidence of spontaneous remission of thoracic nodes compared to the Met-dominant group (78% vs. 33%) at 1-year follow up. ^{18}F-FDG/Met uptake may reflect a differential granulomatous status in sarcoidosis patients, and may be useful for short-term prognostication of patient outcome.

Combination of ^{18}F-FDG and [^{18}F]-α-methyltyrosine (FMT), another amino acid radiotracer with potential used in detecting neoplasm, has been used in a study by Kaira et al (2007) [81]. Twenty-four patients with sarcoidosis who had suspected malignancy underwent both ^{18}F-FDG PET and FMT-PET imaging. The study included 17 patients with extrapulmonary manifestations mimicking malignancy, 3 cancer patients with bilateral hilar lymphadenopathy, and 4 patients with multiple nodules mimicking pulmonary metastases. Increased ^{18}F-FDG uptake with no FMT accumulation was observed in the lymph nodes of all patients.

Figure 9. A) A 24 years old man with cervical and supraclavicular lymphadenopathy. A: Increased ^{18}F-FDG uptake was observed in bilateral hilar, mediastinal, supraclavicular, cervical and abdominal paraaortic lymph nodes (arrows). B) Corresponding lesions does not show increased ^{18}F-FMT uptake. C) CT reveals the ^{18}F-FDG-avid lesions correspond to the systemic lymph nodes (arrows). Noncaseating granuloma was revealed in histopathology examination of the lymph node. The patient remains clinically stable for 14 months after the initial diagnosis, and the lymphadenopathy has disappeared. (Reprinted, with permission, from reference 81).

All extranodal lesions such as spleen, liver and bone marrow were positive on ^{18}F-FDG PET and negative on FMT-PET. No neoplasm was detectedin these sites of radiotracer uptake in all patients. The authors suggested use of FMT-PET in combination with ^{18}F-FDG PET may be useful to distinguish sarcoidosis from malignancy (Fig. 9).

Somatostatin receptors have been identified in vitro within granuloma macrophages, epithelioid cells, and giant cells of sarcoidosis tissue [83]. Kwekkeboom et al (1998) [84] performed [^{111}In]-pentetreotide scintigraphy in 46 patients with sarcoidosis, and demonstrated radiotracer uptake inmediastinal, hilar, and lung sites in 36 of 37 patients with disease involvement in these locations. Pathological uptake of radiotracer in the parotid glands during somatostatin receptor imaging was correlated with higher serum ACE levels. These data suggest that there may be a potential role for other ^{68}Ga-labeled somatostatin receptor radiotracers for use with PET/CT imaging to detect and localize sites of sarcoidosis activity.

Quantitation of global metabolic activity

Image segmentation and global disease assessment enhance the accuracy of measurements made by ^{18}F-FDG PET imaging [85, 86]. Assessment of whole body metabolic burden of disease has been described in the literature for the purpose of quantifying total disease activity in the body [85-91]. The calculation of global metabolic activity is based upon multiplying SUVmean or partial volume corrected SUVmean (PVC-SUVmean) of an organ or lesion of interest by its volume as obtained from anatomical imaging modalities (CT/MRI) or segmentation algorithms use PET images, and then summing across all organs and/or lesions of interest. This latter sum is termed total lesion glycolysis (TLG) or total metabolic volumetric product (MVP).

The concept was first introduced by Alavi et al (1981) [92] for the assessment of the brain in Alzheimer's disease patients and age-matched controls. The authors found that by multiplying segmented brain volumes measured from MRI by mean cerebral glucose metabolic rates, significant differences between two groups could be demonstrated. By combining these measurements in the entire body for various pathological states, one can calculate the global metabolic activity of the underlying process. This approach can be effectively applied in studies involving cancer, atherosclerosis, cardiac disease, and inflammation. The same investigators have proposed a similar approach for assessing global organ function and overall disease activity in other settings [93-99]. Larson et al (1999) [85] was the first to report application of this approach in cancer patients. They quantified changes of pre and post-treatment ^{18}F-FDG PET also called delta TLG or Larson-Ginsberg Index (LGI), expressed as percent response in 41 oncologic patients. The author found that delta TLG showed greater mean changes than SUV maximum or average. Kim et al (2013) [87] demonstrated that TLG is a better predictor for survivals in diffuse large B cell lymphoma patients who are treated with R-CHOP as compared with the International Prognostic Index. However, there is a growing body of evidence supporting the application of volumetric PET/CT parameters in malignancies. Limited studies are available about the application of these indices in non-malignant diseases [85, 87-91, 100]. Abdulla et al (2014) [26]

have applied this concept in patients with non-small cell lung cancer who had radiation pneumonitis after treatment. The authors found that global lung parenchymal glycolysis was significantly increased following radiotherapy in the ipsilateral lung parenchyma whereas no significant change was observed in the contralateral lung. Saboury et al (2014) [98] showed robust correlation between quantitative ^{18}F-FDG PET parameters and clinical and endoscopic surrogate markers of disease activity of Crohn's Disease. As sarcoidosis is also a systemic inflammatory disease and can present in multiple lesions and organs, a global metabolic assessment by employing TLG and MAV may provide potentially useful biomarkers to quantify sarcoidosis activity and to tailor patient treatment. Figure 10 shows whole-body PET/CT images with global quantitative assessment.

Imaging by PET/MRI

Combination of PET and MRI has been developed to improve the correlation between functional and anatomical imaging. MR imaging has major strengths compared with CT, including multiplanar image acquisition , superior soft-tissue contrast resolution, and functional imaging capability through specialized

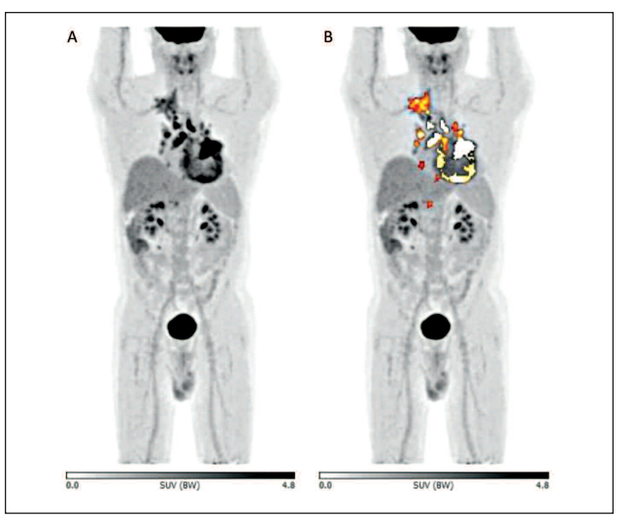

Figure 10. A) Maximum intensity projection of whole-body ^{18}F-FDG PET showed increased ^{18}F-FDG uptake at myocardial, mediastinal and bilateral hilar lymphadenopathy. B) Quantification of PET after segmentation of lesion by an adaptive contrast oriented thresholding algorithem.

Location	SUVmax	SUVmean	MAV (cm^3)	TLG
Heart	4.9	4.8	66.1	319.8
Lymph nodes	5.3	3.4	75.3	256.9
Whole body	5.3	4.1	141.4	576.7

approaches such as diffusion-weighted (DW) imaging, diffusion-tensor imaging, MR elastography, MR spectroscopy and the availability of some targeted MR imaging contrast agents [101, 102]. Many studies suggested new application of PET/MRI in oncology [101, 103-106], neurology [107-110], musculoskeletal disease [111-113] and cardiovascular diseases [114-116]. PET/MRI may have a potential role in sarcoidosis especially for cardiac sarcoidosis and neurosarcoidosis which MRI provides better delineation of anatomical structure than CT (Fig. 11).

Summary

Imaging by ^{18}F-FDG PET provides accurate quantitative assessment of inflammatory activity in patients with sarcoidosis. Furthermore, ^{18}F-FDG PET shows a higher sensitivity than

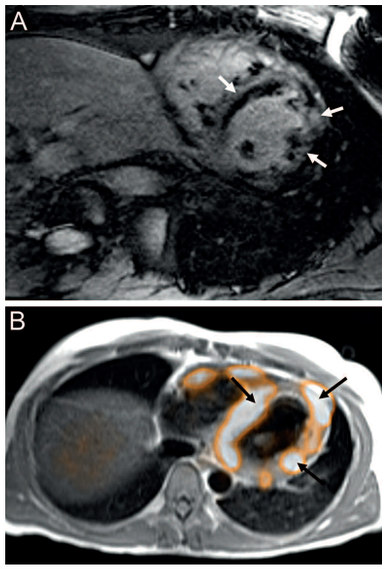

Figure 11. A 51 years old man with history of cardiac sarcoidosis and dysrhythmias. A) Short-axis 1.5-T delayed-phase postcontrast phase-sensitive inversion-recovery gradient-echo MR image of heart reveals heterogeneous regions of delayed enhancement (arrows) in mid- and subepicardial portions of left ventricular myocardium, consistent with granulomatous and/or fibrotic tissue. B) Software-fused ^{18}F-FDG PET/MR image of heart demonstrates heterogeneously increased ^{18}F-FDG uptake (arrows) in left ventricular myocardium (Reprinted and modified, with permission, from reference 102).

^{67}GaC scintigraphy for assessment of the degree and extent of disease activity in patients with sarcoidosis, with the additional advantages of a lower radiation exposure and a shorter delay time between radiotracer administration and image acquisition. Although MRI seems to be the modality of choice for detection and localization of cardiac sarcoidosis and neurosarcoidosis, it may be not able to distinguish inactive from active lesions due to sarcoidosis, potentially leading to difficulties in therapeutic planning. In addition, ^{18}F-FDG PET can be utilized in patients who have contraindications to undergo MRI or to receive gadolinium-based contrast agents. Overall, ^{18}F-FDG PET may play an important role for lesion detection, identification of accessible biopsy sites, quantification of levels of disease activity, prognostication of patient outcome, and determination of response assessment in patients with sarcoidosis. For patients with concomitant malignancy, dual radiotracer PET imaging using ^{18}F-FDG and FMT may successfully discriminate lesions due to sarcoidosis from those due to malignancy. Future larger scale research studies may be performed to further elucidate the role of PET imaging in the management of patients with sarcoidosis.

The authors declare that they have no conflicts of interest.

Bibliography

1. Statement on Sarcoidosis. *American Journal of Respiratory and Critical Care Medicine* 1999; 160: 736-55. 10.1164/ajrccm.160.2.ats4-99 10.1164/ajrccm.160.2.ats4-99.
2. Hem E. [Multiple benign sarcoid of the skin-100 years since Caesar Boeck's pioneering article]. *Tidsskrift for den Norske laegeforening* 1999; 119: 4567-9.
3. Pietinalho A, Hiraga Y, Hosoda Y et al. The frequency of sarcoidosis in Finland and Hokkaido, Japan. A comparative epidemiological study. *Sarcoidosis* 1995; 12: 61-7.
4. Hamzeh N. Sarcoidosis. *The Medical clinics of North America* 2011; 95: 1223-34. 10.1016/j.mcna.2011.08.004 10.1016/j.mcna.2011.08.004.
5. Iannuzzi MC, Rybicki BA, Teirstein AS. Sarcoidosis. *N Engl J Med* 2007; 357: 2153-65. 10.1056/NEJMra071714 10.1056/NEJMra071714.
6. Haimovic A, Sanchez M, Judson MA, Prystowsky S. Sarcoidosis: a comprehensive review and update for the dermatologist: part I. Cutaneous disease. *J Am Acad Dermatol* 2012; 66(5): 699 e1-18; quiz 717-8. S0190-9622(12)00109-0 [pii]. 10.1016/j.jaad.2011.11.965 [doi] S0190-9622(12)00109-0 [pii]. 10.1016/j.jaad.2011.11.965 [doi].
7. Iannuzzi MC, Fontana JR. Sarcoidosis: clinical presentation, immunopathogenesis, and therapeutics. *JAMA* 2011; 305(4): 391-9. 305/4/391 [pii]. 10.1001/jama.2011.10 [doi] 305/4/391 [pii]. 10.1001/ jama.2011.10 [doi].
8. Oki M, Saka H, Kitagawa C et al. Real-time endobronchial ultra sound-guided transbronchial needle aspiration is useful for diagnosing sarcoidosis. *Respirology* 2007; 12: 863-8. 10.1111/j.1440-1843.2007.01145.x 10.1111/j.1440-1843.2007.01145.x.
9. Navani N, Booth HL, Kocjan G et al. Combination of endobronchial ultrasound-guided transbronchial needle aspiration with standard bronchoscopic techniques for the diagnosis of stage I and stage II pulmonary sarcoidosis. *Respirology* 2011; 16(3): 467-72. 10.1111/j.1440-1843. 2011.01933.x [doi] 10.1111/j.1440-1843.2011.01933.x [doi].
10. Costabel U, Ohshimo S, Guzman J. Diagnosis of sarcoidosis. *Current opinion in pulmonary medicine* 2008; 14: 455-61. 10.1097/MCP.0b013e3283056a61 10.1097/MCP.0b013e3283056a61.
11. Kwee TC, Torigian DA, Alavi A. Oncological applications of positron emission tomography for evaluation of the thorax. *J Thorac Imaging* 2013; 28: 11-24. 10.1097/RTI.0b013e318279449b 10.1097/RTI.0b013e318279449b.
12. Youssef G, Leung E, Mylonas I et al. The use of ^{18}F-FDG PET in the diagnosis of cardiac sarcoidosis: a systematic review and metaanalysis including the Ontario experience. *J Nucl Med* 2012; 53: 241-8. 10.2967/jnumed.111.090662 10.2967/jnumed.111.090662.
13. Kwee TC, Torigian DA, Alavi A. Nononcological applications of positron emission tomography for evaluation of the thorax. *J Thorac Imaging* 2013; 28(1): 25-39. 10.1097/RTI.0b013e31827882a9 [doi]. 00005382-201301000-00006 [pii] 10.1097/RTI.0b013e31827882a9 [doi]. 00005382-201301000-00006 [pii].
14. Miyara M, Amoura Z, Parizot C et al. The immune paradox of sarcoidosis and regulatory T cells. *J Exp Med* 2006; 203: 359-70. 10.1084/jem.20050648 10.1084/jem.20050648.
15. O'Neill LA, Hardie DG. Metabolism of inflammation limited by AMPK and pseudo-starvation. *Nature* 2013; 493: 346-55. 10.1038/nature11862 10.1038/nature11862.
16. Osman S, Danpure HJ. The use of 2-[^{18}F]fluoro-2-deoxy-D-glucose as a potential in vitro agent for labelling human granulocytes for clinical studies by positron emission tomography. International journal of radiation applications and instrumentation Part B. *Nuclear medicine and biology* 1992; 19: 183-90.
17. Kubota R, Yamada S, Kubota K et al. Intratumoral distribution of fluorine-18-fluorodeoxyglucose in vivo: high accumulation in macrophages and granulation tissues studied by microautoradiography. *J Nucl Med* 1992; 33: 1972-80.
18. Tahara T, Ichiya Y, Kuwabara Y et al. High [^{18}F]-fluorodeoxyglucose uptake in abdominal abscesses: a PET study. *J Comput Assist Tomogr* 1989; 13(5): 829-31.
19. Sasaki M, Ichiya Y, Kuwabara Y et al. Ringlike uptake of [^{18}F]FDG in brain abscess: a PET study. *J Comput Assist Tomogr* 1990; 14: 486-7.
20. Bissonnette R, Tardif JC, Harel F et al. Effects of the tumor necrosis factor-alpha antagonist adalimumab on arterial inflammation assessed by positron emission tomography in patients with psoriasis: results of a randomized controlled trial. *Circulation Cardiovascular imaging* 2013; 6: 83-90. 10.1161/CIRCIMAGING.112.975730 10.1161/CIRCIMAGING.112.975730.
21. Yarasheski KE, Laciny E, Overton ET et al. ^{18}FDG PET-CT imaging detects arterial inflammation and early atherosclerosis in HIV-infected adults with cardiovascular disease risk factors. *Journal of Inflammation* 2012; 9: 26. 10.1186/1476-9255-9-26 10.1186/1476-9255-9-26.
22. Blomberg BA, Akers SR, Saboury B et al. Delayed time-point ^{18}F-FDG PET CT imaging enhances assessment of atherosclerotic plaque in flammation. *Nucl Med Commun* 2013; 34(9): 860-7. 10.1097/MNM.0b013e3283637512 [doi] 10.1097/MNM.0b013e3283637512 [doi].
23. Subramanian S, Tawakol A, Burdo TH et al. Arterial inflammation in patients with HIV. *JAMA* 2012; 308(4): 379-86. 1221700 [pii]. 10.1001/jama.2012.6698 [doi] 1221700 [pii]. 10.1001/jama.2012.6698 [doi].
24. Dweck MR, Jones C, Joshi NV et al. Assessment of valvular calcification and inflammation by positron emission tomography in patients with aortic stenosis. *Circulation* 2012; 125: 76-86. 10.1161/CIRCULATIONAHA.111.051052 10.1161/CIRCULATIONAHA.111.051052.
25. Yamashita H, Kubota K, Takahashi Y et al. Similarities and differences in fluorodeoxyglucose positron emission tomography/computed tomography findings in spondyloarthropathy, polymyalgia rheumatica and rheumatoid arthritis. *Joint Bone Spine* 2013; 80: 171-7. 10.1016/j.jbspin.2012.04.006 10.1016/j.jbspin.2012.04.006.
26. Abdulla S, Salavati A, Saboury B et al. Quantitative assessment of global lung inflammation following radiation therapy using FDG PET/CT: a pilot study. *Eur J Nucl Med Mol Imaging* 2014; 41: 350-6. 10.1007/s00259-013-2579-4 10.1007/s00259-013-2579-4.
27. Vos FJ, Bleeker-Rovers CP, Oyen WJ. The use of FDG-PET/CT in patients with febrile neutropenia. *Seminars in nuclear medicine* 2013; 43: 340-8. 10.1053/j.semnuclmed.2013.04.007 10.1053/j.semnuclmed.2013.04.007.
28. Balan A, Hoey ET, Sheerin F et al. Multi-technique imaging of sarcoidosis. *Clin Radiol* 2010; 65: 750-60. 10.1016/j.crad.2010.03.014 10.1016/j.crad.2010.03.014.
29. Scadding JG. Sarcoidosis, with Special Reference to Lung Changes. *Br Med J* 1950; 1(4656): 745-53.
30. Oberstein A, von Zitzewitz H, Schweden F, Muller-Quernheim J. Non invasive evaluation of the inflammatory activity in sarcoidosis with high-resolution computed tomography. *Sarcoidosis Vasc Diffuse Lung Dis* 1997; 14: 65-72.
31. Mana J. Nuclear imaging. ^{67}Gallium, ^{201}thallium, ^{18}F-labeled fluoro-2-deoxy-D-glucose positron emission tomography. *Clin Chest Med* 1997; 18(4): 799-811.
32. Sulavik SB, Spencer RP, Weed DA et al. Recognition of distinctive patterns of gallium-67 distribution in sarcoidosis. *J Nucl Med* 1990; 31: 1909-14.
33. Sulavik SB, Spencer RP, Palestro CJ et al. Specificity and sensitivity of distinctive chest radiographic and/or ^{67}Ga images in the noninvasive diagnosis of sarcoidosis. *Chest* 1993; 103: 403-9.
34. Mana J, Gamez C. Molecular imaging in sarcoidosis. *Current opinion in pulmonary medicine* 2011; 17: 325-31. 10.1097/MCP. 0b013e3283480d36 10.1097/MCP.0b013e3283480d36.
35. Jain V, Hasselquist S, Delaney MD. PET scanning in sarcoidosis. *Ann N Y Acad Sci* 2011; 1228: 46-58. 10.1111/j.1749-6632.2011.06075.x [doi] 10.1111/j.1749-6632.2011.06075.x [doi].
36. Nishiyama Y, Yamamoto Y, Fukunaga K et al. Comparative evaluation of ^{18}F-FDG PET and ^{67}Ga scintigraphy in patients with sarcoidosis. *J Nucl Med* 2006; 47: 1571-6. 47/10/1571 [pii] 47/10/1571 [pii].
37. Lewis PJ, Salama A. Uptake of fluorine-18-fluorodeoxyglucose in sarcoidosis. *J Nucl Med* 1994; 35: 1647-9.
38. Braun JJ, Kessler R, Constantinesco A, Imperiale A. ^{18}F-FDG PET/CT in sarcoidosis management: review and report of 20 cases. *Eur J Nucl Med Mol Imaging* 2008; 35: 1537-43. 10.1007/s00259-008-0770-9 10.1007/s00259-008-0770-9.
39. Teirstein AS, Machac J, Almeida O et al. Results of 188 whole-body fluorodeoxyglucose positron emission tomography scans in 137 patients with sarcoidosis. *Chest* 2007; 132: 1949-53. 10.1378/chest.07-1178 10.1378/chest.07-1178.
40. Mostard RL, Voo S, van Kroonenburgh MJ et al. Inflammatory activity assessment by F18 FDG-PET/CT in persistent symptomatic sarcoidosis. *Respiratory medicine* 2011; 105: 1917-24. 10.1016/j.rmed.2011.08.01210.1016/j.rmed.2011.08.012.
41. Rubini G, Cappabianca S, Altini C et al. Current clinical use of FDG-PET/CT in patients with thoracic and systemic sarcoidosis. *Radiol Med* 2014; 119(1): 64-74. 10.1007/s11547-013-0306-7 [doi] 10.1007/s11547-013-0306-7 [doi].

42. Sobic-Saranovic DP, Grozdic IT, Videnovic-Ivanov J et al. Responsiveness of FDG PET/CT to treatment of patients with active chronic sarcoidosis. *Clin Nucl Med* 2013; 38(7): 516-21. 10.1097/RLU.0b013e31828731f5[doi] 10.1097/RLU.0b013e31828731f5 [doi].
43. Sobic-Saranovic D, Grozdic I, Videnovic-Ivanov J et al. The utility of ^{18}F-FDG PET/CT for diagnosis and adjustment of therapy in patients with active chronic sarcoidosis. *J Nucl Med* 2012; 53:1543-9. 10.2967/jnumed.112.10438010.2967/jnumed. 112.104380.
44. Muller NL, Mawson JB, Mathieson JR et al. Sarcoidosis: correlation of extent of disease at CT with clinical, functional, and radiographic findings. *Radiology* 1989; 171: 613-8. 10.1148/radiology.171.3. 2717730 10.1148/radiology.171.3.2717730.
45. Jain V, Hasselquist S, Delaney MD. PET scanning in sarcoidosis. *Ann N Y Acad Sci* 2011; 1228: 46-58. 10.1111/j.1749-6632.2011.06075.x 10.1111/j.1749-6632.2011.06075.x.
46. Keijsers RG, Verzijlbergen FJ, Oyen WJ et al. ^{18}F-FDG PET, genotype-corrected ACE and sIL-2R in newly diagnosed sarcoidosis. *Eur J Nucl Med Mol Imaging* 2009; 36: 1131-7. 10.1007/s00259-009-1097-x 10.1007/s00259-009-1097-x.
47. Keijsers RG, Grutters JC, van Velzen-Blad H et al. ^{18}F-FDG PET patterns and BAL cell profiles in pulmonary sarcoidosis. *Eur J Nucl Med Mol Imaging* 2010; 37: 1181-8. 10.1007/s00259-009-1376-6 10.1007/s00259-009-1376-6.
48. Keijsers RG, Verzijlbergen JF, van Diepen DM et al. ^{18}F-FDG PET in sarcoidosis: an observational study in 12 patients treated with inflix imab. *Sarcoidosis Vasc Diffuse Lung Dis* 2008; 25: 143-9.
49. Mostard RL, Verschakelen JA, van Kroonenburgh MJ et al. Severity of pulmonary involvement and ^{18}F-FDG PET activity in sarcoidosis. *Respir Med* 2013; 107(3):439-47. S0954-6111(12)00422-2 [pii]. 10.1016/j.rmed.2012.11.011 [doi] S0954-6111(12)00422-2 [pii]. 10.1016/j.rmed.2012.11.011 [doi].
50. Ambrosini V, Zompatori M, Fasano L et al. ^{18}F-FDG PET/CT for the assessment of disease extension and activity in patients with sarcoidosis: results of a preliminary prospective study. *Clin Nucl Med* 2013; 38(4): e171-7. 10.1097/RLU.0b013e31827a27df [doi] 10.1097/RLU.0b013e31827a27df [doi].
51. Cooper LT, Baughman KL, Feldman AM et al. The role of endomyocardial biopsy in the management of cardiovascular disease: a sci entific statement from the American Heart Association, the American College of Cardiology, and the European Society of Cardiology Endorsed by the Heart Failure Society of America and the Heart Failure Association of the European Society of Cardiology. *Eur Heart J* 2007; 28: 3076-93. ehm456 [pii]. 10.1093/eurheartj/ehm456 [doi] ehm456 [pii]. 10.1093/eurheartj/ehm456 [doi].
52. Tahara N, Tahara A, Nitta Y et al. Heterogeneous myocardial FDG up take and the disease activity in cardiac sarcoidosis. *JACC Cardiovas cular imaging* 2010; 3: 1219-28. 10.1016/j.jcmg.2010.09.015 10.1016/j.jcmg.2010.09.015.
53. Ohira H, Tsujino I, Ishimaru S et al. Myocardial imaging with ^{18}F-fluoro-2-deoxyglucose positron emission tomography and magnetic resonance imaging in sarcoidosis. *Eur J Nucl Med Mol Imaging* 2008; 35: 933-41. 10.1007/s00259-007-0650-8 10.1007/s00259-007-0650-8.
54. Langah R, Spicer K, Gebregziabher M, Gordon L. Effectiveness of pro longed fasting ^{18}F-FDG PET-CT in the detection of cardiac sarcoidosis. *J Nucl Cardiol* 2009; 16: 801-10. 10.1007/s12350-009-9110-0 10.1007/s12350-009-9110-0.
55. Okumura W, Iwasaki T, Toyama T et al. Usefulness of fasting ^{18}F-FDG PET in identification of cardiac sarcoidosis. *J Nucl Med 2004*; 45: 1989-98. 45/12/1989 [pii] 45/12/1989 [pii].
56. Ishimaru S, Tsujino I, Takei T et al. Focal uptake on ^{18}F-fluoro-2-deoxyglucose positron emission tomography images indicates cardiac involvement of sarcoidosis. *Eur Heart J 2005*; 26: 1538-43.10.1093/eurheartj/ehi180 10.1093/eurheartj/ehi180.
57. Yamagishi H, Shirai N, Takagi M et al. Identification of cardiac sarcoidosis with ^{13}N-NH^3/^{18}F-FDG PET. *J Nucl Med* 2003; 44: 1030-6.
58. Keijsers RG, Verzijlbergen FJ, Rensing BJ, Grutters JC. Cardiac sarcoidosis: a challenge to measure disease activity. *J Nucl Cardiol* 2008; 15: 595-8. 10.1016/j.nuclcard.2008.02.033 10.1016 /j.nuclcard.2008.02.033.
59. Matthews R, Bench T, Meng H et al. Diagnosis and monitoring of cardiac sarcoidosis with delayed-enhanced MRI and ^{18}F-FDG PET-CT. *J Nucl Cardiol* 2012; 19: 807-10. 10.1007/s12350-012-9550-9 10.1007/s12350-012-9550-9.
60. Casset-Senon D, Philippe L, Renard JP, Cosnay P. Recurrent ventricular tachycardia in cardiac sarcoidosis: usefulness of fluorodeoxyglucose positron emission tomography for adequate management of corticoid therapy after placement of an implantable cardioverter defibrillator. *J Nucl Cardiol* 2008; 15: 282-5. 10.1016/j.nuclcard.2008.01.006 10.1016/j.nuclcard.2008.01.006.
61. Takeda N, Yokoyama I, Hiroi Y et al. Positron emission tomography predicted recovery of complete A-V nodal dysfunction in a patient with cardiac sarcoidosis. *Circulation* 2002; 105: 1144-5.
62. Mc Ardle BA, Leung E, Ohira H et al. The role of F(18)-fluorodeoxyglucose positron emission tomography in guiding diagnosis and management in patients with known or suspected cardiac sarcoidosis. *J Nucl Cardiol* 2013; 20: 297-306. 10.1007/s12350-012-9668-9 10.1007/s12350-012-9668-9.
63. Skali H, Schulman AR, Dorbala S. ^{18}F-FDG PET/CT for the assessment of myocardial sarcoidosis. *Curr Cardiol Rep* 2013; 15(4): 352. 10.1007/s11886-013-0352-8 [doi] 10.1007/s11886-013-0352-8 [doi].
64. Morooka M, Moroi M, Uno K et al. Long fasting is effective in inhibiting physiological myocardial ^{18}F-FDG uptake and for evaluating active lesions of cardiac sarcoidosis. *EJNMMI Res* 2014; 4(1): 1. 2191-219X-4-1 [pii]. 10.1186/2191-219X-4-1 [doi] 2191-219X-4-1 [pii]. 10.1186/2191-219X-4-1 [doi].
65. Dubey N, Miletich RS, Wasay M et al. Role of fluorodeoxyglucose positron emission tomography in the diagnosis of neurosarcoidosis. *J Neurol Sci* 2002; 205: 77-81. S0022510X02002253 [pii] S0022510X02002253 [pii].
66. Bolat S, Berding G, Dengler R et al. Fluorodeoxyglucose positron emission tomography (FDG-PET) is useful in the diagnosis of neurosarcoidosis. *J Neurol Sci* 2009; 287: 257-9. 10.1016/j.jns.2009.08.060 10.1016/j.jns.2009.08.060.
67. Meenakshi M, Arnold C, Broadley SA. The value of [^{18}F]-fluorodeoxyglucose-positron emission tomography/CT scanning in the diagnosis of neurosarcoidosis. *J Clin Neurosci* 2012; 19: 1461-2. 10.1016/j.jocn.2012.02.013 10.1016/j.jocn.2012.02.013.
68. Bartels S, Kyavar L, Blumstein N et al. FDG PET findings leading to diagnosis of neurosarcoidosis. *Clin Neurol Neurosurg* 2013; 115: 85-8. 10.1016/j.clineuro.2012.03.042 10.1016/j.clineuro.2012.03.042.
69. Asabella AN, Gatti P, Notaristefano A et al. F-18 FDG PET/CT in the diagnosis of a rare case of neurosarcoidosis in a patient with diabetes insipidus. *Clin Nucl Med* 2011; 36: 795-7. 10.1097/RLU.0b013e318219b28b 10.1097/RLU.0b013e318219b28b.
70. Aide N, Benayoun M, Kerrou K et al. Impact of [^{18}F]-fluorodeoxyglucose ([^{18}F]-FDG) imaging in sarcoidosis: unsuspected neurosarcoidosis discovered by [^{18}F]-FDG PET and early metabolic response to corticosteroid therapy. *Br J Radiol* 2007; 80: e67-71.10.1259 /bjr/33076108 10.1259/bjr/33076108.
71. Huang JF, Aksamit AJ, Staff NP. MRI and PET imaging discordance in neurosarcoidosis. *Neurology* 2012; 79: 1070. 10.1212/WNL.0b013e3182684672 10.1212/WNL.0b013e3182684672.
72. Flanagan EP, Hunt CH, Lowe V et al. [^{18}F]-fluorodeoxyglucose-positron emission tomography in patients with active myelopathy. *Mayo Clinic proceedings* 2013; 88: 1204-12. 10.1016/j.mayocp.2013.07.019 10.1016/j.mayocp.2013.07.019.
73. Sakushima K, Yabe I, Shiga T et al. FDG-PET SUV can distinguish be tween spinal sarcoidosis and myelopathy with canal stenosis. *J Neurol* 2011; 258: 227-30. 10.1007/s00415-010-5729-7 10.1007/s00415-010-5729-7.
74. Keijsers RG, Verzijlbergen EJ, van den Bosch JM et al. ^{18}F-FDG PET as a predictor of pulmonary function in sarcoidosis. *Sarcoidosis Vasc Diffuse Lung Dis* 2011; 28(2): 123-9.
75. Umeda Y, Demura Y, Morikawa M et al. Prognostic value of dual-time-point ^{18}F-fluorodeoxyglucose positron emission tomography in patients with pulmonary sarcoidosis. *Respirology* 2011; 16(4): 713-20. 10.1111/j.1440-1843.2011.01966.x [doi] 10.1111/j.1440-1843.2011.01966.x [doi].
76. Vorselaars AD, Verwoerd A, van Moorsel CH et al. Prediction of relapse after discontinuation of infliximab therapy in severe sarcoidosis. *Eur Respir J* 2014; 43(2): 602-9. 09031936.00055213 [pii].10.1183/09031936.00055213 [doi] 09031936.00055213 [pii].10.1183/09031936.00055213 [doi].
77. Blankstein R, Osborne M, Naya M et al. Cardiac positron emission tomography enhances prognostic assessments of patients with suspected cardiac sarcoidosis. *J Am Coll Cardiol* 2014; 63(4): 329-36. S0735-1097(13)05455-7 [pii]. 10.1016/j.jacc.2013.09.022 [doi] S0735-

1097(13)05455-7 [pii]. 10.1016/j.jacc.2013.09.022 [doi].
78. Osborne MT, Hulten EA, Singh A et al. Reduction in ^{18}F-fluorodeoxyglucose uptake on serial cardiac positron emission tomography is associated with improved left ventricular ejection fraction in patients with cardiac sarcoidosis. *J Nucl Cardiol* 2014; 21(1): 166-74. 10.1007/s12350-013-9828-6 [doi] 10.1007/s12350-013-9828-6 [doi].
79. Reich JM. Neoplasia in the etiology of sarcoidosis. *Eur J Intern Med* 2006; 17: 81-7. 10.1016/j.ejim.2005.09.023 10.1016/j.ejim.2005.09. 023.
80. Reich JM, Mullooly JP, Johnson RE. Linkage analysis of malignancy-associated sarcoidosis. *Chest* 1995; 107: 605-13.
81. Kaira K, Oriuchi N, Otani Y et al. Diagnostic usefulness of fluorine-18-alpha-methyltyrosine positron emission tomography in combination with ^{18}F-fluorodeoxyglucose in sarcoidosis patients. *Chest* 2007; 131: 1019-27. 10.1378/chest.06-2160 10.1378/chest.06-2160.
82. Yamada Y, Uchida Y, Tatsumi K et al. Fluorine-18-fluorodeoxyglucose and carbon-11-methionine evaluation of lymphadenopathy in sarcoidosis. *J Nucl Med* 1998; 39: 1160-6.
83. ten Bokum AM, Hofland LJ, de Jong G et al. Immunohistochemical localization of somatostatin receptor sst2A in sarcoid granulomas. *Eur J Clin Invest* 1999; 29: 630-6. eci498 [pii] eci498 [pii].
84. Kwekkeboom DJ, Krenning EP, Kho GS et al. Somatostatin receptor imaging in patients with sarcoidosis. *Eur J Nucl Med* 1998; 25: 1284-92.
85. Larson SM, Erdi Y, Akhurst T et al. Tumor Treatment Response Based on Visual and Quantitative Changes in Global Tumor Glycolysis Using PET-FDG Imaging. The Visual Response Score and the Change in Total Lesion Glycolysis. *Clin Positron Imaging* 1999; 2: 159-71.
86. Alavi A, Newberg AB, Souder E, Berlin JA. Quantitative analysis of PET and MRI data in normal aging and Alzheimer's disease: atrophy weighted total brain metabolism and absolute whole brain metabolism as reliable discriminators. *J Nucl Med* 1993; 34: 1681-7.
87. Kim TM, Paeng JC, Chun IK et al. Total lesion glycolysis in positron emission tomography is a better predictor of outcome than the International Prognostic Index for patients with diffuse large B cell lymphoma. *Cancer* 2013; 119: 1195-202. 10.1002/cncr.27855 10. 1002/cncr.27855.
88. Heijmen L, de Geus-Oei LF, de Wilt JH et al. Reproducibility of functional volume and activity concentration in ^{18}F-FDG PET/CT of liver metastases in colorectal cancer. *Eur J Nucl Med Mol Imaging* 2012; 39: 1858-67. 10.1007/s00259-012-2233-6 10.1007/s00259-012-2233-6.
89. Chen HH, Chiu NT, Su WC et al. Prognostic value of whole-body total lesion glycolysis at pretreatment FDG PET/CT in non-small cell lung cancer. *Radiology* 2012; 264: 559-66. 10.1148/radiol.12111148 10.1148/radiol.12111148.
90. Lim R, Eaton A, Lee NY et al. ^{18}F-FDG PET/CT metabolic tumor volume and total lesion glycolysis predict outcome in oropharyngeal squamous cell carcinoma. *J Nucl Med* 2012; 53: 1506-13. 10.2967/jnumed.111. 101402 10.2967/jnumed.111.101402.
91. Yoo J, Choi JY, Moon SH et al. Prognostic significance of volume-based metabolic parameters in uterine cervical cancer determined using ^{18}F-fluorodeoxyglucose positron emission tomography. *Intern J Gynecol Cancer* 2012; 22: 1226-33. 10.1097/IGC.0b013e31826 0a905 10.1097/IGC.0b013e318260a905.
92. Alavi A, Reivich M, Greenberg J et al. Mapping of functional activity in brain with ^{18}F-fluoro-deoxyglucose. *Seminars in nuclear medicine* 1981; 11: 24-31.
93. Berkowitz A, Basu S, Srinivas S et al. Determination of whole-body metabolic burden as a quantitative measure of disease activity in lymphoma: a novel approach with fluorodeoxyglucose-PET. *Nucl Med Commun* 2008; 29: 521-6. 10.1097/MNM.0b013e3282f813a4 10.1097/MNM.0b013e3282f813a4.
94. Bural GG, Torigian DA, Burke A et al. Quantitative assessment of the hepatic metabolic volume product in patients with diffuse hepatic steatosis and normal controls through use of FDG-PET and MR imaging: a novel concept. *Mol Imaging Biol* 2010; 12: 233-9.10.1007/s11307-009-0258-4 10.1007/s11307-009-0258-4.
95. Nawaz A, Saboury B, Basu S et al. Relation between popliteal-tibial artery atherosclerosis and global glycolytic metabolism in the affected diabetic foot: a pilot study using quantitative FDG-PET. *J Amer Podiatr Med Assoc* 2012; 102: 240-6. 102/3/240 [pii] 102/3/240 [pii].
96. Mehta NN, Torigian DA, Gelfand JM et al. Quantification of atherosclerotic plaque activity and vascular inflammation using [18-F] fluorodeoxyglucose positron emission tomography/computed tomography (FDG-PET/CT). Journal of visualized experiments : *JoVE* 2012; 63: e3777. 10.3791/3777 10.3791/3777.
97. Hernandez-Martinez A, Marin-Oyaga VA, Salavati A et al. Quantitative assessment of global hepatic glycolysis in patients with cirrhosis and normal controls using ^{18}F-FDG-PET/CT: a pilot study. *Ann Nucl Med* 2014; 28: 53-9. 10.1007/s12149-013-0780-y 10.1007/s12149-013-0780-y.
98. Saboury B, Salavati A, Brothers A et al. FDG PET/CT in Crohn's disease: correlation of quantitative FDG PET/CT parameters with clinical and endoscopic surrogate markers of disease activity. *Eur J Nucl Med Mol Imaging* 2014; 41(4): 605-14. 10.1007/s00259-013-2625-2 10.1007/s00259-013-2625-2.
99. Salavati A, Saboury B, Alavi A. Comment on: "Tumor Aggressiveness and Patient Outcome in Cancer of the Pancreas Assessed by Dynamic ^{18}F-FDG PET/CT". *J Nucl Med* 2014; 55(2): 350-1.10.2967/jnumed.113.130138 10.2967/jnumed.113.130138.
100. Salavati A, Basu S, Heidari P, Alavi A. Impact of fluorodeoxyglucose PET on the management of esophageal cancer. *Nucl Med Commun* 2009; 30: 95-116. 10.1097/MNM.0b013e32831af20410.1097/MNM.0b013e32831af204.
101. Kwee TC, Basu S, Saboury B et al. Functional oncoimaging techniques with potential clinical applications. *Frontiers in bioscience (Elite edition)* 2012; 4: 1081-96.
102. Torigian DA, Zaidi H, Kwee TC et al. PET/MR imaging: technical aspects and potential clinical applications. *Radiology* 2013; 267: 26-44. 10.1148/radiol.13121038 10.1148/radiol.13121038.
103. Ahmed Shamim S, Torigian DA, Kumar R. PET, PET/CT, and PET/MR Imaging Assessment of Breast Cancer. *PET Clinics* 2008; 3: 381-93.
104. Hustinx R, Torigian DA, Namur G. Complementary Assessment of Abdominopelvic Disorders with PET/CT and MRI. *PET Clinics* 2008; 3: 435-49.
105. Katz S, Ferrara T, Alavi A, Torigian DA. PET, CT, and MR Imaging for Assessment of Thoracic Malignancy: Structure Meets Function. *PET Clinics* 2008; 3: 395-410.
106. Goldberg MF, Chawla S, Alavi A et al. PET and MR Imaging of Brain Tumors. *PET Clinics* 2008; 3: 293-315.
107. Boss A, Bisdas S, Kolb A et al. Hybrid PET/MRI of intracranial masses: initial experiences and comparison to PET/CT. *J Nucl Med* 2010; 51: 1198-205.10.2967/jnumed.110.074773 10.2967/jnumed.110.074773.
108. Schwenzer NF, Stegger L, Bisdas S et al. Simultaneous PET/MR imaging in a human brain PET/MR system in 50 patients-current state of image quality. *Eur J Radiol* 2012; 81: 3472-8. 10.1016/j.ejrad.2011.12.027 10.1016/j.ejrad.2011.12.027.
109. Cho ZH, Son YD, Kim HK et al. Observation of glucose metabolism in the thalamic nuclei by fusion PET/MRI. *J Nucl Med* 2011; 52: 401-4. 10.2967/jnumed.110.081281 10.2967/jnumed.110.081281.
110. Salamon N, Kung J, Shaw SJ et al. FDG-PET/MRI coregistration improves detection of cortical dysplasia in patients with epilepsy. *Neurology* 2008; 71: 1594-601. 10.1212/01.wnl.0000334752.41807.2f 10.1212/01.wnl.0000334752.41807.2f.
111. Nawaz A, Torigian DA, Siegelman ES et al. Diagnostic performance of FDG-PET, MRI, and plain film radiography (PFR) for the diagnosis of osteomyelitis in the diabetic foot. *Mol Imaging Biol* 2010; 12: 335-42. 10.1007/s11307-009-0268-2 10.1007/s11307-009-0268-2.
112. El-Haddad G, Kumar R, Pamplona R, Alavi A. PET/MRI depicts the exact location of meniscal tear associated with synovitis. *Eur J Nucl Med Mol Imaging* 2006; 33: 507-8. 10.1007/s00259-005-0034-x 10.1007/s00259-005-0034-x.
113. Miese F, Scherer A, Ostendorf B et al. Hybrid ^{18}F-FDG PET-MRI of the hand in rheumatoid arthritis: initial results. *Clinical Rheumatology* 2011; 30: 1247-50. 10.1007/s10067-011-1777-3 10.1007/s10067-011- 1777-3.
114. Syed IS, Feng D, Harris SR et al. MR imaging of cardiac masses. *Magn Reson Imaging Clin N Am* 2008; 16: 137-64. vii. 10.1016/j.mric.2008.02.009 10.1016/j.mric.2008.02.009.
115. Probst S, Seltzer A, Spieler B et al. The appearance of cardiac metastasis from squamous cell carcinoma of the lung on F-18 FDG PET/CT and post hoc PET/MRI. *Clin Nucl Med* 2011; 36: 311-2. 10.1097/RLU.0b013e31820a9fd1 10.1097/RLU.0b013e31820a9fd1.
116. Nensa F, Poeppel TD, Beiderwellen K et al. Hybrid PET/MR imaging of the heart: feasibility and initial results. *Radiology* 2013; 268: 366-73. 10.1148/radiol.13130231 10.1148/radiol.13130231.